Acta Cryst. (1977). A**33**, 288–293

Variable-Path Laue Measurements and Extinction

BY J. L. LAWRENCE

School of Physical Sciences, University of St Andrews, North Haugh, St Andrews, KY16 9SS, Scotland

AND A. MCL. MATHIESON

Division of Chemical Physics, CSIRO, PO Box 160, *Clayton, Victoria, Australia* 3168

(*Received* 17 *August* 1976; *accepted* 6 *October* 1976)

A simple experimental procedure is described for the correction of secondary extinction by the symmetrical Laue method with a parallel-sided plate specimen. The method is based on the work of Bragg, James & Bosanquet [*Phil. Mag.* (1921), **42**, 1–17] but, unlike their method, it requires the use of only a single specimen. The X-ray beam path through the specimen is changed by tilt of the specimen. Instead of one measurement of intensity for a given path length, a set of four or eight measurements for different paths is taken. The divergence within the sets and the trend of the mean value with change of path length provide diagnostics as to the extinction state and the level of homogeneity in the specimen. Extrapolation to zero path yields the value for Q', the effective integrated reflecting power per unit volume, corrected for absorption and average secondary extinction. The measurements can be placed on an absolute basis and an estimate of the magnitude of the mean primary extinction made. Results are presented for a plate of LiF.

Introduction

Although it is virtually axiomatic that the effect of 'secondary' extinction is functionally dependent on the beam path-length, there has been little investigation of the Laue (transmission) method of measuring integrated intensity using progressive and controlled change in the X-ray beam path through single-crystal specimens. The main records of systematic study of this type relate to the early work of Bragg, James & Bosanquet (1921*b*) on specimens of NaCl and a subsequent investigation by Bragg & West (1928) on topaz. These studies involved a series of parallel-sided plates of differing thickness. Measurements on plates of quartz as well as wedge-shaped specimens of that material were carried out by Sakisaka (1927). In the case of earlier work by Lawrence (1972), limited use of different paths through the specimen of LiF was made to investigate equivalent reflexions.

Investigations of this type would appear to warrant further exploration in order to aid in understanding the extinction state of crystals and hence assist in assessing the scope of transmission methods for establishing structure-factor values. The angle-setting capabilities of the modern diffractometer, combined with the increased precision of modern counters, provide an excellent basis for re-opening this neglected area.

The intention in the present paper is to present a preliminary exploration to indicate the potential of the method rather than to attempt to provide accurate numerical data.

Method

Principle

The standard Laue method in the symmetrical mode (*International Tables for X-ray Crystallography*, 1959, pp. 265, 291) involves equation (1), in which ϱ' is the integrated intensity, E is the total diffracted intensity, ω the angular scan rate of the specimen, I_0 the incident energy flux, t' the effective total path of incident plus diffracted beams, μ' the effective attenuation coefficient and Q' the effective integrated reflecting power per unit volume.

$$\varrho' = E\omega/I_0 = Q't' \exp(-\mu't') \tag{1}$$

$$\ln(\varrho'/t') = \ln Q' - \mu't'. \tag{1a}$$

The usual procedure involves a single measurement of each reflexion, corresponding to a single value of t'. From this measurement, application of equation (1) yields an estimate of Q', provided an appropriate value of μ' is available from other experiments. μ' is equal to $\mu_0(\lambda)$, the normal absorption coefficient, only in the limit $Q' \rightarrow 0$ [see Calvert, Killean & Mathieson (1976)].

Following recognition of 'extinction' effects in their reflexion measurements on NaCl (Bragg, James & Bosanquet, 1921*a*) these authors introduced (1921*b*) the method of making a series of Laue (transmission) measurements (in the symmetrical mode) on samples of differing thickness cut from the same specimen. They plotted the data in the form $\ln(\varrho'/t')$ *versus* t' (equation 1*a*). They did not, however, use the intensity data so measured to derive *prima facie* values of Q'. Instead, they used the measurements to extract values of $\mu'(hkl)$, for selected hkl reflexions when in the diffracting position, from the slope of the log plot. These $\mu'(hkl)$ values were used to adjust the reflexion data in order to derive hkl structure-factor values corrected for extinction [specified later as 'secondary', see Bragg & West (1928)]. The efficacy of this step depended on the implied assumption that the values of μ' established for the crystal interior (Laue case) were directly applicable to the intensity measurement for the surface (Bragg

case). There was therefore a measure of ambiguity arising from the mixing of results from the different procedures.

While offering potential improvement in measurement technique, use of a series of n slices has certain practical disadvantages, the more obvious being as follows:

(i) The different slices are derived from different parts of the original specimen. While it is necessarily assumed that this specimen is uniform in its interior, there may be, in practice, significant variation from slice to slice.

(ii) Each slice has to be ground parallel-sided and its individual thickness determined, *i.e.* $2n$ surfaces to be ground and n dimensions measured. The preparation of $2n$ surfaces to virtually equivalent condition presents a difficult task.

(iii) The ratio of the depth of the surface layer to that of the unchanged interior is dependent (*a*) on the extent of the grinding and (*b*) on the total thickness of the specimen. As the total thickness decreases, the ratio of surface layer to interior increases.

Some of these disadvantages may be minimized or eliminated by making use of the inbuilt flexibility of the modern diffractometer.

With a parallel-sided single-crystal plate specimen of thickness, t, a variety of X-ray beam paths can be selected by appropriate tilt of the specimen while the diffraction condition is still retained (Fig. 1*a*). For example, if one is dealing with a crystal which is mounted so that the c^* axis (say) is parallel to the φ axis of the diffractometer, the path length of the incident plus diffracted beams is $t' = pt(\cos\theta_l)^{-1}$, where θ_l is the Bragg angle for the $00l$ reflexion and the value of $p[=(\cos\varphi)^{-1}]$ is established by the appropriate adjustment of φ. Various p-multiples of the basic path $t(\cos\theta_l)^{-1}$ can be set, up to a practical limit determined by the lateral dimensions of the specimen. Also, instead of a single measurement for each crystal slice, as in the standard procedure, there are potentially eight positions for each tilt value of the specimen, for all of which the path length of incident plus diffracted beams is the same. Fig. 1(*b*) shows the paths for the various φ settings.

Advantages gained with the use of a single specimen are as follows:

(i) There are only two surfaces to be prepared.

(ii) The uniformity of thickness and the actual value of the mean t need only be established for the one specimen.

(iii) A group of eight measurements is easily carried out by the appropriate setting of φ together with adequate positive and negative 2θ ranges. If there is a restriction to only positive 2θ, then appropriate complementary settings of χ, *e.g.* 90 and 270°, will permit attainment of the full set. If one is restricted to $+2\theta$ only, on a quarter-circle χ instrument, then only four measurements are possible without remounting of the specimen.

(iv) Any dimensional non-uniformities should be recognizable by consideration of variations within the set. The average of the eight measurements in a set will tend to minimize individual deviations.

For details of establishing the reference origin of φ see Lawrence & Mathieson (1976), who used the tilt procedure for the measurement of attenuation coefficient.

Operational procedure

The single-crystal material was LiF, the dimensions of the specimen being $20 \times 20 \times 1{\cdot}283$ (2) mm. The radiation used was Mo $K\alpha$, monochromated by a pyrolytic graphite crystal. Measurements of integrated intensity from the specimen were made on a Siemens diffractometer. Limitations in the range of χ and of access to the -2θ region restricted measurement to four

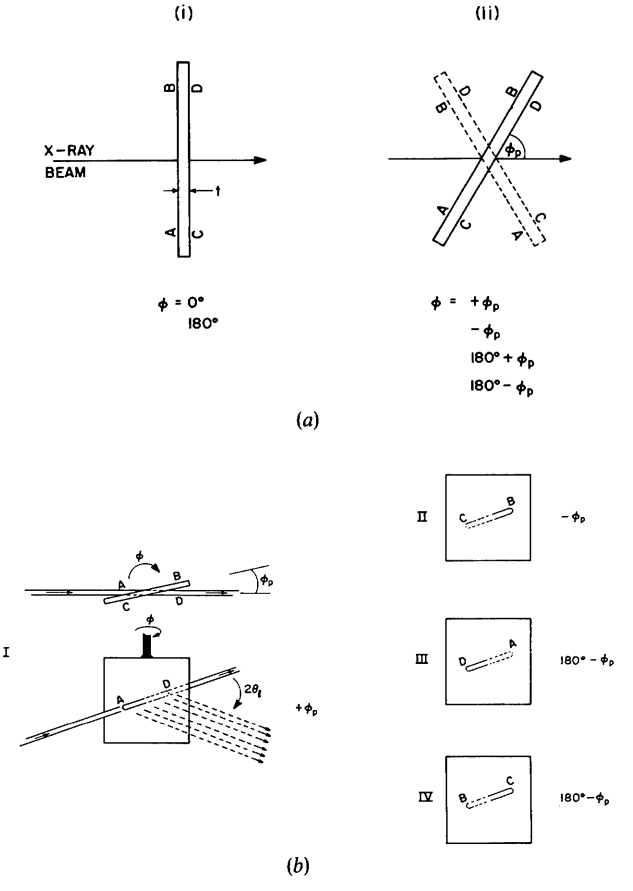

Fig. 1. (*a*) Projection of the incident and diffracted beams in the diffracting plane showing the tilt procedure to increase the path by adjustment of φ. (i) The two positions for $\varphi = 0$ and 180°. (ii) The four positions for $\varphi = \pm\varphi_p$ and $180° \pm \varphi_p$. These correspond to a $\chi = 90°$ setting. Another set of four can be obtained at $\chi = 270°$. (*b*) The paths through the crystal slice for one setting of χ. For one value of $(\cos\varphi)^{-1}$, the paths of the incident and diffracted beams are shown in I. For the other three tilt positions II, III, and IV, the incident beam path is illustrated. Entrant and exit regions are as if seen from above and are differentiated by solid and dashed lines.

rather than to the full potential of eight members of a set. Measurements were made at a series of values of p. For the higher orders, physical limitations restricted the range of p. In general, $p(\cos\theta_l)^{-1}$ was terminated just beyond 5. For the measurement of integrated intensity, the total time for each scan was adjusted to maintain reasonable standard deviation values consistent with the overall stability of the system.

The measurements of integrated intensity were made on an absolute basis.* The procedure used was to select ω so that E and I_0 were of approximately similar magnitude, with appropriate time adjustment. The determination of $\omega = \Delta\theta/\Delta t$ in the case of a step-scan, as for the Siemens diffractometer, is simply reduced to the establishment of an angle interval, $\Delta\theta$, and a time interval, Δt, the accuracy of both of which can be high so that the precision of E and I_0 determines the final accuracy of ϱ'. Certain variants in the more usual procedure for absolute measurement were introduced to avoid (i) the use of absorbers and (ii) any change in specimen surface interposed in the beam path. Concerning item (i), the radiation used should ideally be monochromatic, but if there are any short-wavelength components, their contribution to the measured intensity is significantly enhanced by the use of absorbers. So it is advisable to adjust the X-ray generator voltage to avoid excitation of $\lambda/2$ radiation and to set the output so that with no absorbers, apart from the specimen, in the beam path, count rates are at reasonable levels to avoid serious levels of lost counts. On item (ii), the normal procedure to allow measurement of I_0 is to remove the specimen. This means that the procedures for measurement of E and of I_0 differ significantly in that one involves the interposition of the specimen in the beam while the other does not. To eliminate this difference, the measurement of I_0 can be made with the specimen plate in place but not in the diffracting position. A series of measurements is made of the direct beam, I_p, with different thicknesses of specimen, $t' = pt$, by adjustment of tilt angle, φ, and the plot of $\ln I_p$ against p extrapolated to $p=0$ (see Lawrence & Mathieson, 1976). This yields a value for I_0 under conditions essentially similar to that involved in the measurement of E.

Absolute values of ϱ' for 002, 004 and 006 at $p=1{\cdot}0$ were established by this means. The measurements for 008 and 0,0,10 were, by cross-reference, also placed on an absolute basis.

* We refer here to absolute measurement of integrated intensity and not to methods of placing structure factors, from intensity data, on an absolute scale. The two are only synonymous under an extinction-free regime.

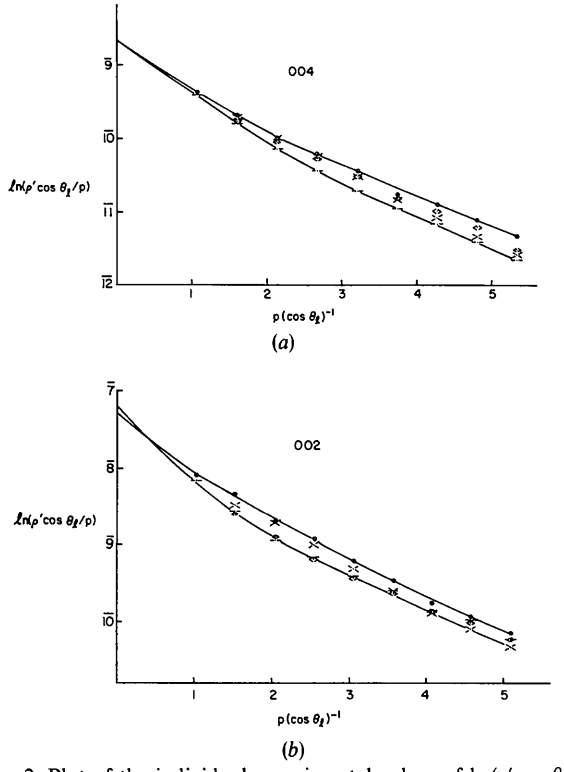

Fig. 2. Plot of the individual experimental values of $\ln(\varrho'\cos\theta_l/p)$ *versus* $p(\cos\theta_l)^{-1}$; (*a*) 004; (*b*) 002. Extrapolation of the envelope of values to $p(\cos\theta_l)^{-1}=0$, *i.e.* equivalent to zero thickness, is illustrated.

Results

The experimental data are plotted as $\ln(\varrho'\cos\theta_l/p)$ *versus* $p(\cos\theta_l)^{-1}$ in Figs. 2 and 3.

There are two aspects of the measurements which should be noted: (i) the divergence of the values within a set for a given path length (four measurements in the present case) and (ii) the trend of the envelope of the data sets and of the set average with change of path length.

For 0,0,10, the numerical data show only small divergence within each set, not sufficient to be revealed in the log plots on the scale used. They are of the order of 2%. The level of divergence gradually increases with increasing level of interaction, *i.e.* effective diffracting power, Q', in 008 and 006 so that for 004 and 002, Fig. 2, the values within a set show considerable divergence. Certain observations may be made at this stage concerning the latter two reflexions. First, the ϱ' values for a given sense of tilt, Fig. 2(*a*), *e.g.* those designated by a short straight line, display a trend which, in general, is no longer linear but is curved. This pattern of curvature is not, however, clearcut, there being considerable scatter in certain runs, *e.g.* those identified by the carets $\langle\,\rangle$ in Fig. 2(*b*). The overall trend is, however, clear. Second, the runs associated with different specific tilt-senses all tend to asymptote to the same value at $p=0$. This tendency is more obvious if one considers the envelopes of values for the two reflexions. This overall pattern is held to more closely for 004, Fig. 2(*a*), than for 002, Fig. 2(*b*), a feature on which comment is offered below.

If, following the indications of the envelope of values, we provisionally accept the average value of

$\ln(Q' \cos\theta_l/p)$ for a set of paths as physically significant, then the results for the five orders with variations of p are displayed in Fig. 3. 0,0,10 and 008 appear to be acceptably linear (apart from one outlier point for 008). The two low-order reflexions, 004 and 002, are obviously non-linear, being curved concave upwards. In respect of 004, extrapolation to $p(\cos\theta_l)^{-1}=0$ does not allow a wide variation (see the envelope extrapolation in Fig. 2). For 002, the curvature in the small-p region is significantly greater than that for 004 and it is evident that its clearer definition would require further data points. Extrapolation is therefore less certain but an approximate value can be established which is sufficient to illustrate the basic aim of this paper.

The case of 006 is intermediate. Visual inspection of the five orders in Fig. 3 would suggest that there is likely to be a measure of curvature at low p for this reflexion and such a curvature has been sketched in the figure. Strictly speaking, the measurement data can be fitted adequately to a straight line. So, for this case, the two possible extrapolations are recorded.

Since the data have been made on an absolute scale, the value of the extrapolation to $p(\cos\theta_l)^{-1}=0$ corresponds to $\ln(Q't)$, and since t has been determined at 1·283 (2) mm, absolute values of Q' can be obtained. These are listed in Table 1. For comparison, values of Q unaffected by extinction, are also listed. These have been calculated from the F_c values in Killean, Lawrence & Sharma (1972).

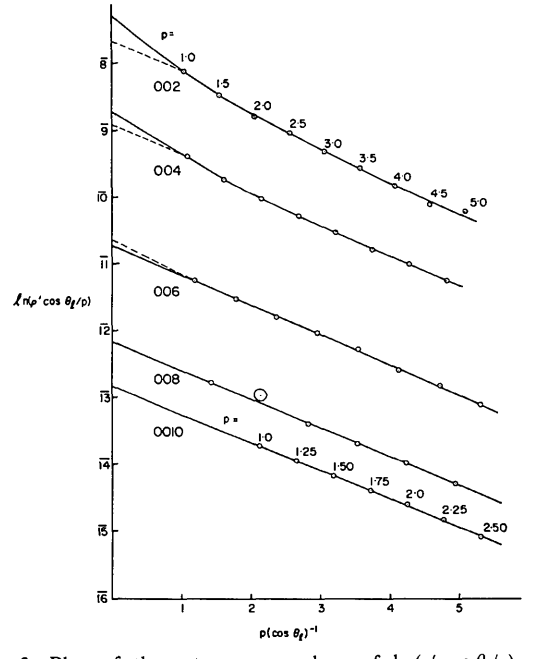

Fig. 3. Plot of the set-average values of $\ln(Q' \cos\theta_l/p)$ *versus* $p(\cos\theta_l)^{-1}$ for the orders 002 to 0·0·10. The curves are extrapolated to $p(\cos\theta_l)^{-1}=0$. For 004 and 002, a dashed straight line of slope $\mu_0(\lambda)t$ is drawn through the values for $p=1$. For 006, two extrapolations are shown. The straight line corresponds to a least-squares fit to the experimental data, a straight-line being assumed to be appropriate. The curved dashed line is based on an analogous trend, correspondingly reduced, obvious in the 004 and 002 orders.

Table 1. *Numerical data derived mainly from Fig.* 3

Column 2 presents the experimental absolute values of $Q'(00l)$ obtained by extrapolation effectively to $t=0$. Column 3 lists the theoretical values corresponding to kinematical, extinction-free conditions. These are derived by calculation from F_c values in Killean, Lawrence & Sharma (1972). The ratio of these values, which gives a measure of the level of primary extinction for the particular reflexion, is given in the next column. Column 5 lists for 002 and 004 the Q' values which would be obtained by simply correcting for absorption the measurements at $p=1$. The last column lists the values of μ' derived from the slope of the straight lines fitted to the data for 0,0,10, 008 and 006. The value of $\mu_0(\lambda)$ derived from this data is shown. For purposes of discussion in the text, values of the slope of the 002 and 004 curves for $p>2{\cdot}0$, assumed to be linear in that region, are also listed in brackets, since their numerical significance is not straightforward.

00*l*	$Q'\times10^6$	$Q\times10^6$	Q'/Q	$Q'_\mu\times10^6$	μ' (cm^{-1})
002	5814	16171	0·360	3531	[4·02 (3)]
004	1325	1466	0·904	1021	[3·55 (2)]
006	183 (168)	195·8	0·935 (0·858)	—	3·47 (2)
008	42·5	44·0	0·966	—	3·32 (3)
0,0,10	21·5	21·6	0·995	—	3·25 (2)

$\mu_0(\lambda)=3{\cdot}20$ (3).

For completeness, the values, by least-squares fit, of the slope against $p(\cos\theta_l)^{-1}$ of the data for 0,0,10, 008 and 006 are listed in Table 1. From these, the $\mu_0(\lambda)$ value for $Q=0$ was derived as 3·20 (3) cm^{-1}. This may be compared with the experimental value of 3·12 (2) cm^{-1} found by Lawrence & Mathieson (1976). Straight-line fits to the data for 004 and 002 using only data for $p=2$ and higher values give μ' values listed in Table 1. They tend to values not markedly different from those for the higher orders. Comment on these results is presented below.

To indicate the relation of these measurements to those obtained by the normal single-measurement Laue procedure, dashed lines of slope $\mu_0(\lambda)t$ have been drawn through the values for $p=1$ for 004 and 002. The intercepts of these lines at $p(\cos\theta_l)^{-1}=0$ correspond to the Laue measurement corrected only for ordinary absorption. The corresponding values of Q'_μ are listed in the second column from the right of Table 1 to show the difference from the curve-extrapolated values.

Interpretation

Discussion of the results is based on equation (2) below, which may be compared with equation 8.4 of Darwin (1922, p. 823) and also equation 71 of Weiss (1966, p. 48), provided that, in the case of the latter, Q' is equated with $Q(1-\frac{1}{3}A^2)$, the factor $(1-\frac{1}{3}A^2)$ being associated with 'primary extinction'.

$$Q'=Q't'[1-\gamma_2(Q't')+\gamma_3(Q't')^2-\gamma_4(Q't')^3 +\ldots]\exp[-\mu_0(\lambda)t']. \quad (2)$$

In situations where there is only 'secondary extinction', $Q'=Q$. The relation in equation (2) can be re-

arranged to that in equation (3) to accord more closely with the data presentation in Figs. 2 and 3, *viz.*

$$\ln(\varrho' \cos\theta_l/p) = \ln\{Q't[1-\gamma_2(Q't')+\gamma_3(Q't')^2 - \gamma_4(Q't')^3+\ldots]\} - \mu_0(\lambda)pt(\cos\theta_l)^{-1}. \quad (3)$$

The results, namely the log plots, for the higher orders 0,0,10 and 008 are characteristic of the situation where the interaction between the incident beam and the crystal is very weak, so that the diffraction from the individual crystallites is effectively from the whole irradiated volume, ΔV, of the crystallite, *i.e.* $Q\Delta V$, where Q is the diffracting power per unit volume when the ideally-imperfect (mosaic) crystal formula is applicable. Under these circumstances, the actual distribution of crystallites is not significant. Second diffraction (γ_2) back into the main beam is small while third diffraction (γ_3) back into the diffracted beam is negligible. The abstraction of energy from the incident beam is dependent essentially only on the volume, and therefore the path, traversed. Hence, for a given path length the different paths show virtually no difference in measured intensity. For this regime, equation (2) is adequately represented by equation (4)

$$\varrho' = Q't' \exp[-\mu_0(\lambda)t'](1-\gamma_2 Q't'). \quad (4)$$

Since Q' is small, $(1-\gamma_2 Q't')$ can be replaced by $\exp(-\Delta\mu' t')$, where $\Delta\mu' = \gamma_2 Q'$. Then $\mu' = \mu_0(\lambda) + \Delta\mu'$, a formula associated with Bragg, James & Bosanquet (1921*b*) [see equation (1) above]. Under these circumstances, the log plot of ϱ'/t' is essentially linear.

As the interaction between the beams and the crystallites increases on moving to reflexions with higher Q' values, the significance of the contributions from the higher-order diffraction processes, γ_3 *etc.*, becomes progressively greater. Since the incident beam, on its passage through the specimen, is being diffracted (and re-diffracted *etc.*) to varying extents by individual crystallites, so that the volume of the crystallites is no longer irradiated uniformly, the end-result – the measured intensity – becomes dependent on the distribution of crystallites along the individual beam path followed. If this distribution is not smooth but discrete then the different paths will be associated with different sets of γ_n coefficients in equation (3) so that the observed intensity is no longer representative of the sample but of the specific path. Not only will the γ_n coefficients have a range of values for different paths but the Q' values may also differ, particularly when Q'/Q is considerably lower than unity. As a result, the intensities for such cases can show a considerable spread, as is evident in the present case.

So each path used will represent a discrete sampling of the paths through the specimen, the divergence of values for a set giving a measure of the sample spread. For a discrete distribution, the average of the four values may not represent an ideal mean but it is likely to be physically more meaningful in relation to other sets than would single values (Figs. 2 and 3).

While the above presents a physical picture of the situation, it is clear that, for the cases where wide divergence within a set is observed, none of the individual values in the general region of p can provide physically definitive values without a knowledge of the discrete population statistic of crystallites. It is only by extrapolation to effectively zero thickness that one can avoid the necessity to determine a series of γ_n parameters. The extrapolated value of Q' derived is corrected for normal absorption and also for 'secondary extinction' effects. In neither case is it necessary to determine absorption or extinction coefficients explicitly.

In the case of 004, the value of Q' obtained by extrapolation is 1325×10^{-6}, which is only marginally smaller than Q (1466×10^{-6}). Since Q'/Q is near to unity, variation of Q' is restricted. Hence only the γ_n coefficients are variable and it is clear that the extrapolations of both the envelope, Fig. 2(*a*), and of the average, Fig. 3, lead to closely similar results.

In the case of 002, the situation is somewhat different. The value of Q' obtained is 5814×10^{-6} whereas the value of Q is 16171×10^{-6}. Hence there is considerable 'primary extinction' and Q'/Q may vary considerably around its mean value 0·360. So, for 002, there may be wide variation of Q' values as well as of γ_n coefficients in equation (2). As a result, the individual tilt runs can be envisaged as extrapolating to Q' values at $p(\cos\theta_l)^{-1}=0$ which cover a range so that the envelope convergence evident for 004 is less obvious for 002 (Fig. 2*b*).

One may note that if, in respect of equation (2), one brought the normal absorption component to the left-hand side together with t', there would remain on the right-hand side the expression

$$Q'[1-\gamma_2(Q't')+\gamma_3(Q't')^2-\gamma_4(Q't')^3\ldots].$$

If the trend of this function with change in t' is considered, it is evident that the slope at $t'=0$ relates to the γ_2 coefficient. As t' increases, the other components of the series progressively grow in size but are of alternate sign so that the curvature decreases and tends to a small value. Obviously the curvature is concave upwards, but the slope of the latter part of the curve is small. This is in accord with the μ' values measured for $p>2{\cdot}0$ for 004 and 002 (Table 1 and Fig. 3).

Discussion

When one considers the capabilities of the variable-path Laue technique, the limited use to which it has been put is somewhat surprising. In the region of low-level interaction the interpretation is relatively straightforward. The linearity of plot establishes that extinction is 'secondary' and extrapolation to zero path length yields effectively kinematical values of Q. From the first experiment by Bragg, James & Bosanquet (1921*b*) on NaCl there has been virtually no exploitation of the technique until recently when Göttlicher & Kieselbach (1976) used a series of LiOH crystal plates to measure structure-factor values free from 'second-

ary' extinction. In both NaCl and LiOH the log plots are effectively linear although the orders measured were associated with 'strong' reflexions. It must be assumed that for the specimens of both these materials, the crystallite distribution must have had a relatively larger angular half-width.

Perhaps one reason for the failure to exploit this technique may be related to the work of Bragg & West (1928) on topaz. These authors measured integrated intensities (single values for each t) for a series of slices with ground faces. The log plot proved to be curved and the authors stated that 'no satisfactory conclusion about the extinction can be drawn'. They associated the effect with a change in the crystal when subjected to the strain set up in the grinding process, and suggested that the surface layers are reduced to the mosaic form by grinding and that the total intensity is due to two contributions, one from the two surfaces (more disordered), the other from the interior (less disordered).

With each specimen slice being given presumably a similar surface-grinding preparation, the ratio of path through surface layer to path through interior was assumed to increase and so also was the ratio of 'mosaic' (surface) to 'perfect' (interior) intensity as the specimen total thickness decreases. It was stated by Bragg & West that this is part of the explanation for the curvature of the log plot in the case of topaz.

In the case of the tilt procedure with a single specimen, the ratios remain constant with tilt. The presence of significant curvature for LiF in Fig. 3 appears to indicate that the contribution from the surface layers is not a critical component in the explanation of the curvature but that it is inherent in the diffraction process when the interaction level, and hence extinction, is high.

Concerning the experiments on topaz, James (1948) states – 'No constant or approximately constant property of the crystal slice is measured by experiments of this kind'. Subsequently, Pringle & Peace (1952) published a brief note disagreeing with this statement and claiming to be able to interpret the data on topaz as due to the existence of 'large secondary extinction'.

The experiment with LiF would suggest that James's statement was unnecessarily pessimistic. While individual measurements may represent only an isolated sample for a discrete statistical spread, the use of sets of measurements with different path lengths allows a more adequate and significant selection. In addition, extrapolation to effective zero specimen thickness tends to eliminate the influence of the multiple-diffraction coefficients, γ_n, and to provide values free of absorption and of 'secondary' extinction.

Summary

The variants of the technique of Bragg, James & Bosanquet (1921*b*) which we have introduced include the following features: (i) use of a single parallel-sided plate specimen, (ii) systematic adjustment of the total length of the incident-plus-diffracted-beam path by tilting the plate, (iii) measurement of sets of integrated intensity involving different paths of equal length, (iv) measurement placed on an absolute intensity basis by an improved procedure and (v) derivation of absolute intensity data free of absorption and of path-dependent 'secondary' extinction by extrapolation to effectively zero path.

The technique has been tested on a specimen of single-crystal lithium fluoride.

The procedure provides diagnostics on the extinction state of the specimen. This study draws attention to the limitations of one-off measurements by contrast with those derived from multiple measurements resulting from change in a variable such as the beam path.

One general comment arises from this work. Any measurement involving a specific path through a real crystal will have an idiosyncratic value. One will only be able to extract from that measurement a physically definitive value if one knows precisely the size of the crystallites, their distribution and sequence – an almost impossible task or at best incapable of yielding precise values. This being the case, the value of *elaboration* of theoretical models of extinction for small crystals may be questioned since a vital assumption underlying such theories (largely because it provides a necessary basis for mathematical treatment) is that the crystal is 'uniform' – namely that, within its surface boundaries, its state is uniform. That this basic assumption is questionable is shown by the present work and, particularly for specimens which have been abraded with intent to produce a sample of a special shape, *e.g.* sphere, by the work of Boehm, Prager & Barnea (1974).

References

Boehm, J. M., Prager, P. R. & Barnea, Z. (1974). *Acta Cryst.* A**30**, 335–337.

Bragg, W. L., James, R. W. & Bosanquet, C. H. (1921*a*). *Phil. Mag.* **41**, 309–337.

Bragg, W. L., James, R. W. & Bosanquet, C. H. (1921*b*). *Phil. Mag.* **42**, 1–17.

Bragg, W. L. & West, J. (1928). *Z. Kristallogr.* **69**, 118–148.

Calvert, L. D., Killean, R. C. G. & Mathieson, A. McL. (1976). *Acta Cryst.* A**32**, 648–652.

Darwin, C. G. (1922). *Phil. Mag.* **43**, 800–829.

Göttlicher, S. & Kieselbach, B. (1976). *Acta Cryst.* A**32**, 185–192.

International Tables for X-ray Crystallography (1959). Vol. II. Birmingham: Kynoch Press.

James, R. W. (1948). *The Optical Principles of the Diffraction of X-rays*. London: Bell.

Killean, R. C. G., Lawrence, J. L. & Sharma, V. C. (1972). *Acta Cryst.* A**28**, 405–407.

Lawrence, J. L. (1972). *Acta Cryst.* A**28**, 400–404.

Lawrence, J. L. & Mathieson, A. McL. (1976). *Acta Cryst.* A**32**, 1002–1004.

Pringle, G. E. & Peace, A. G. (1952). *Nature, Lond.* **169**, 36.

Sakisaka, Y. (1927). *Jap. J. Phys.* **4**, 171–181.

Weiss, R. J. (1966). *X-ray Determination of Electron Distributions*. Amsterdam: North-Holland.